

THE HYDRODYNAMIC PRESSURE FIELD OF THE SHIP ZODIAK, MEASUREMENTS AND CALCULATIONS

JAN BIELAŃSKI

Gdansk University of Technology
Faculty of Ocean Engineering and Ship Technology
Narutowicza 11/12, 80-233 Gdansk, Poland
jbielan@pg.gda.pl

The article presents the results of measurements of the slowly changing hydrodynamic pressure field HPF generated by the movement of the ship, Zodiak, in the Bay of Gdansk. The measurement results have been obtained in the framework of the program of the work in Siramis, under the auspices of the European Defence Administration of the EU, by the research team of the Naval Academy in Gdynia. The measurement results were compared with the results of the calculations using the boundary element method as distribution singularities on the vessel surface and at the bottom of the sea. Also used, in part, were HPF measurements carried out for the ships Kapitan Poinc and Quest, made by the same research team. The results of the measurements made it possible to verify the analytical model for calculating HPF. Then, calculations were made with HPF dimensionless characteristics depending on the ship's speed, the depth of the sea and the distance from the plane of symmetry of the ship.

INTRODUCTION

Last year, studies were made of the hydrodynamic pressure field (HPF) for the oceanographic ship *Zodiak* and a large tug rescue-boat, *Kapitan Poinc*, in the Bay of Gdańsk. The study was conducted within the framework of the research program *Siramis*. As part of the same program the research team of the Naval Academy in Gdynia has carried out HPF research for the ship *Quest*, near Ashau, in Germany. The article was based primarily on the results of the HPF measurements for the ship *Zodiak*, and to some extent the test results were used for the HPF of the ship *Quest*. The HPF results for *Kapitan Poinc* served only to construct the last two drawings.

1. ZODIAK, COMPARISON OF HPF MEASURED IN JULY LAST YEAR ALONG WITH CALCULATIONS

The oceanographic ship *Zodiak* has the following main dimensions: (length, width and draft) = (L, B, T), $L \times B \times T = 57.39 \times 10.83 \times 3.27$ [m], length on waterline $L_{WL} = 57.39$ m, total length $L_{OA} = 61.33$ m and the block coefficient of the hull $C_b = 0.48$. The speed at which the HPF measurements were performed in July last year and the horizontal distance of the ship from the probe IGLOO are shown in Table 1. Column 4 contains the most accurate possible measurement of the horizontal distance from the pressure probe using GPS, while 6 was determined on the basis of the calculated HPF field.

Tab.1.

Time and measurement number on 2013_07_03	Speed [kn]	Speed [m/s]	Distance from IGLOO AIS [m]	Distance from IGLOO AIS [m] GPS-ASG [m]	Calculated distance from IGLOO [m]	Calculated distance from IGLOO-correlated with the exact GPS [m]
column number	1	2	3	4	5	6
10_47_02, No.1	6,3	3.238	19	16	16	11.55
10_57_41, No.2	6,1	3.135	5	4,5	12	7.55
11_08_18, No.3	8,5	4.369	6,5	8,3	11,5	7.05
11_16_14, No.4	8,2	4.215	5	3,9	11	6.55
11_25_52, No.5	10,5	5.397	18	15,1	18	13.55
11_33_41, No.6	10,1	5.191	5	1,7	10,5	6.05
11_41_59, No.7	6,2	3,187	12	11,4	14	9.55
12_00_54, No.8	5,6	2.878	7	0,6	10,5	6.05
12_14_03, No.9	5,8	2.981	19	16,9	15	10.55

Below are only the results of measurements and calculated HPF for the minimum speed of the ship with a bottom depth $H = 10$ m and a deep pressure of around $H_1 = 9$ m:



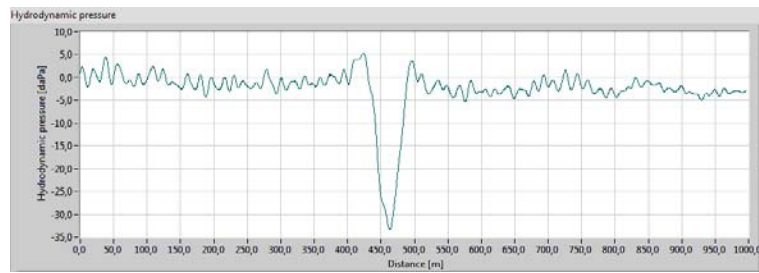


Fig. 1. HPF measurement results for vessel *Zodiak* at a bottom depth of 10m and a speed of 5.8 knots, No.9 in table 1.

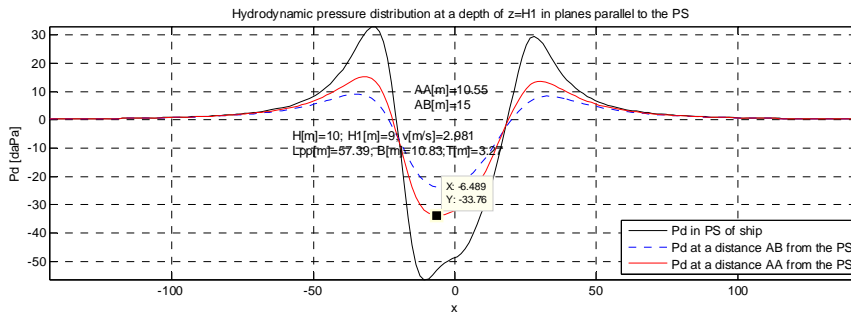


Fig. 2. HPF calculated results for vessel *Zodiak* at a bottom depth of 10m and a deep pressure of around 9m, a speed of 5.8 knots, No.9 in table 1.

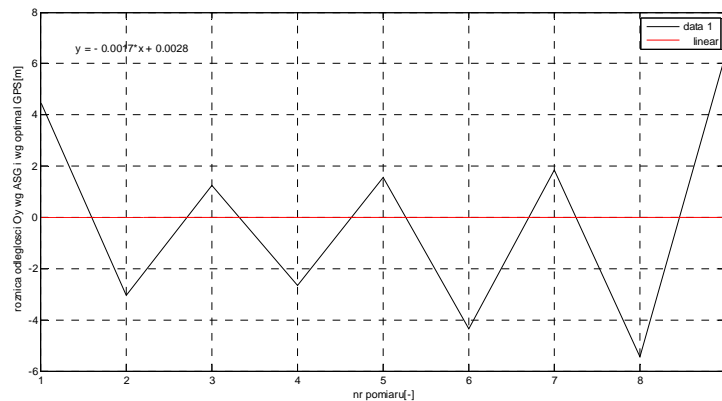


Fig. 3. Graph of the difference in value of the columns 4 and 6 from table 1 in a linear approximation.

It was only after the measurement and analysis of the results that the research team was informed that the GPS antenna was not positioned in the plane of symmetry, but on the side of the wheelhouse. This is shown in Figure 3.

2. ZODIAK, COMPARISON OF THE HPF MEASURED IN MAY LAST YEAR ALONG WITH CALCULATIONS

Similarly, as for the measurements in July, the speed at which the measurements of HPF were performed in May of last year and the horizontal distance of the ship from the probe IGLOO are all shown in Table 2.

Tab.2.

Time and measurement number on 2013_05_15	Speed [kn]	Speed [m/s]	Distance from IGLOO AIS [m]	Calculated distance from IGLOO [m]	The numbers of measurements by increasing the speed
column number	1	2	3	4	5
13_27_11, No.1	5,9	3.033	50	25	4
13_49_42, No.2	6,1	3.14	30	15	5
14_07_35, No.3	7,7	3.96	8	13	7
14_25_29, No.4	10,2	5.24	8	10.5	9
14_56_15, Fig.5	4,9	2.52	3,5	3	1
15_13_33, No.6	7,5	3.86	1,5	7	6
15_30_47, No.7	9,3	4.78	3,5	3	8
16_01_33, No.8	5	2.57	13	21	2
16_12_18, No.9	5,7	2.93	8	9	3

Below are only the results of measurements and the calculated HPF for the minimum speed of the ship with a bottom depth of $H = 10\text{m}$ and a deep pressure of around $H1 = 9\text{m}$:

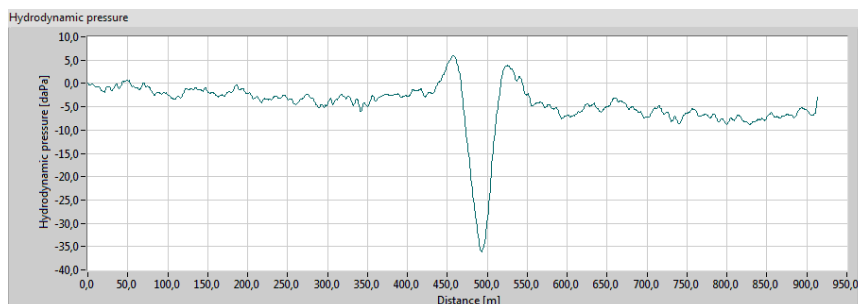


Fig.4. HPF measurement results for vessel *Zodiak* at a bottom depth of 10m and a speed of 4.9 knots, No.5 in table 2.

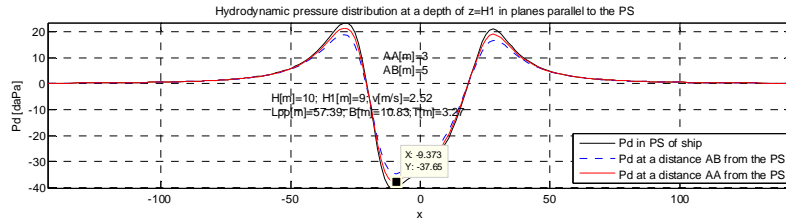


Fig. 5. HPF calculated results for vessel *Zodiak* at a bottom depth of 10m and a deep pressure of around 9m, a speed of 4.9 knots, No.5 in table 2.

The results of the HPF measurements for *Zodiak* were obtained by one probe. In addition, with regard to the shift of the GPS antenna on board, the results are consistent with the calculations in terms of the low pressure peak of the HPF. Minor compatibility is obtained for the length of the low pressure peak and the high pressure at the stern and the bow. In order to verify these characteristics, a hydrodynamic pressure field used the results of the field measurements made by the research team from the Naval Academy of Gdynia for the vessel *Quest*.

3. COMPARISON OF THE MEASURED AND CALCULATED HYDRODYNAMIC PRESSURE FIELD OF THE VESSEL *QUEST*

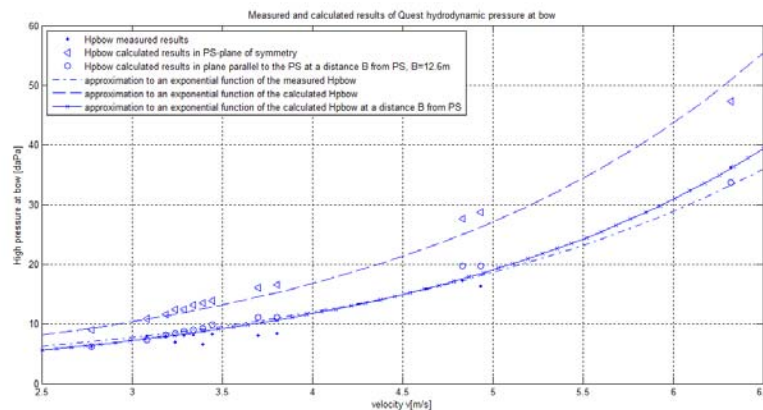


Fig.6. Measured results of high pressure at bow H_{pbow} and calculated H_{pbow} on a plane of symmetry PS and on the plane at a distance of $B=12.6m$ from the PS.

As mentioned above, the research team of the Naval Academy of Gdynia carried out HPF research of the ship *Quest* near Ashau, in Germany.

Figure 6 summarizes the results of the calculations and measurements of high pressure on the bow. These calculations were performed on a plane of symmetry and at a distance of $B = 12.6\text{m}$ from the ship. This first PS is indicated by triangles and the latter by wheels. The measurement results are indicated by dots. Furthermore, the dashed line approximations give three kinds of data.

The approximating curve measurements of pressures have a good consistency and are calculated at a distance of B from the PS. However, for low and medium speeds, the measured results are below the curve-B, and for higher speeds, above the curve. For speeds of less than 10 knots the approximating curves, curve-B and the measurement curve, are all very close to each other.

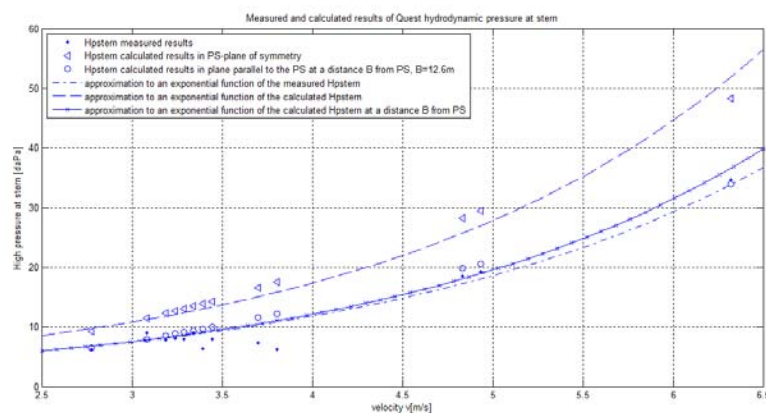


Fig. 7. Measured results of high pressure at the stern $H_{p\text{stern}}$ and calculated $H_{p\text{stern}}$ on the plane of symmetry PS and the a plane at a distance of $B=12.6\text{m}$ from the PS.

The same situation as above for the high pressure at the bow which we can see in Figure, 6 we also have in Figure 7, where the high pressure at the stern has been presented.

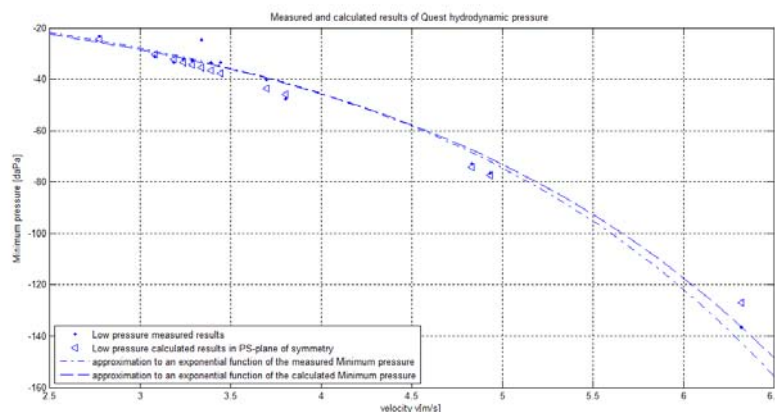


Fig. 8. Measured results of low pressure $H_{p\text{low}}$ and calculated $H_{p\text{low}}$ on the plane of symmetry PS and the approximated curves.

Illustrated in Figure 8, the curves approximating the measured and calculated low pressure $H_{p\text{low}}$ overlap in a large speed range.

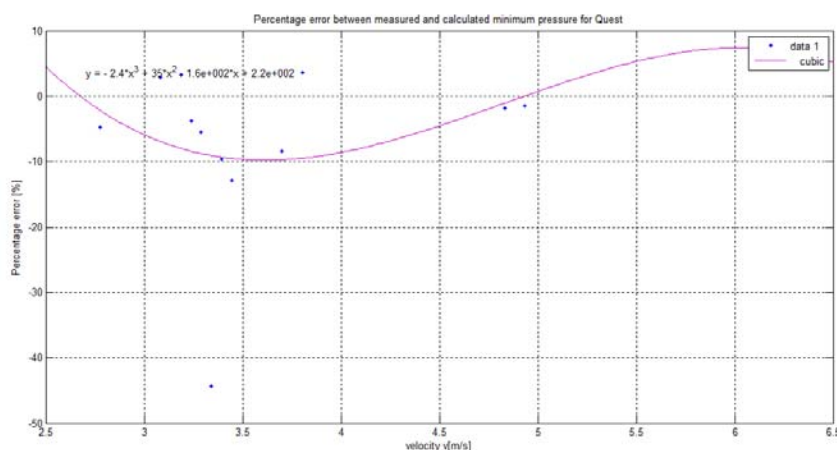


Fig. 9. The percentage difference between the measured and calculated low pressure $H_{p\text{low}}$ for the ship *Quest*.

The approximated curve of the third degree distribution of the percentage difference between measured and calculated low pressure shows that this difference does not exceed a 10% error.

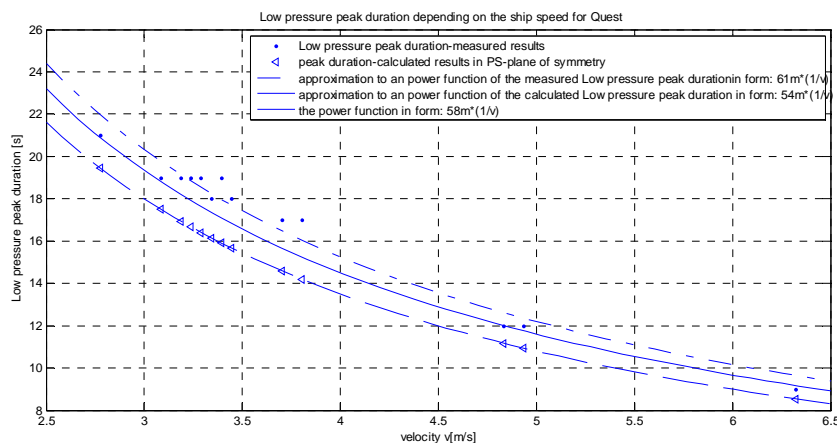


Fig. 10. Low pressure peak duration as a function of ship speed.

The measured and calculated low pressure peak duration is approximated to a power function in the forms a) - $(61m)/v$ and c) - $(54m)/v$, respectively. The curve between them is in form (b) - $(58m)/v$. The measurement points are contained between curves (b) and $(64m)/v$. The *Quest's* vessel length on a waterline is approximately $L_{wL}=72m$. A value of $54m$ from the (c) curves represents 75% of the L_{wL} and $61m$ from the (a) curves represents 85% of the L_{wL} . However $58m$ from (b) represents 80% of the L_{wL} . For a low speed of the ship, the measuring points revolve around a curve (a) and for high-speeds around curve (b). The coefficients of the power functions of the measured low pressure peak duration changes its value from 85%

to 80% L_{WL} and approaches curve (c). These coefficients in these functions represent the length of the low pressure peak of the vessel *Quest*. The calculations have a constant value equal to 54m, the measurement value decreases from 61m to 58m-57m, with an increasing of the speed ship for a constant depth of the sea of $H = 22$ m. Whether this is a real phenomenon reducing the length of the low pressure peak or just less accurate readings of measurements, we do not know.

4. THE DIMENSIONLESS HYDRODYNAMIC PRESSURE FIELD OF THE VESSEL *QUEST* AT HIGH SPEEDS AND THE INFLUENCE OF THE DRIFT VELOCITY ON THIS

These are the results of the HPF calculation of the vessel *Quest* for the velocity $V_x=12.3kn=6.322m/s$. The drift speed of the ship is $V_y=0$.

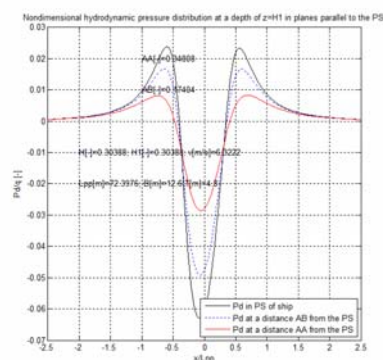


Fig. 11. Dimensionless hydrodynamic pressure distribution on the plane of symmetry (PS plane Oxz) of the ship and in planes parallel to the PS at a distance of AB and AA from the PS. Ship speed is $V_x=6.322m/s$, and without drift, $V_y=0$.

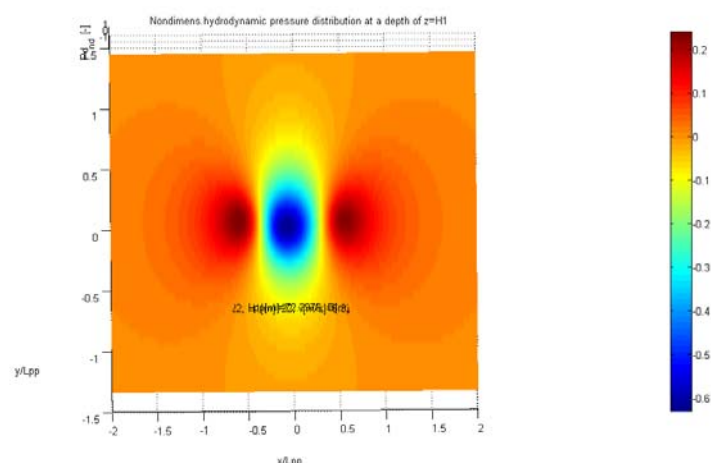


Fig. 12. The hydrodynamic pressure field of *Quest* in a plane Oxy parallel to the bottom of the sea. Ship speed is $V_x=6.322m/s$, and without drift, $V_y=0$.

These are the results of calculations with the same speed of $V_x=6.322\text{m/s}$ and with a drifting speed of $V_y=0.1\text{m/s}$. This drift velocity corresponds to the angular velocity of the ship $\omega=2\pi/T = 2.763\text{e-}3\text{rad/s} = 0.158\text{deg/s}$ and the time required for a full rotation of the ship is $T=37.9\text{min}$.

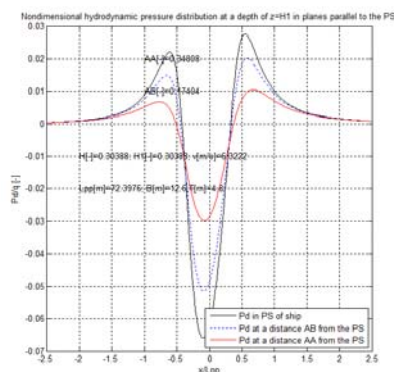


Fig. 13. Dimensionless hydrodynamic pressure distribution on the plane of symmetry (PS plane Oxz) of the ship and on planes parallel to the PS at a distance of AB and AA from the PS. Ship speed is $V_x=6.322\text{m/s}$, with a drifting speed of $V_y=0.1\text{m/s}$.

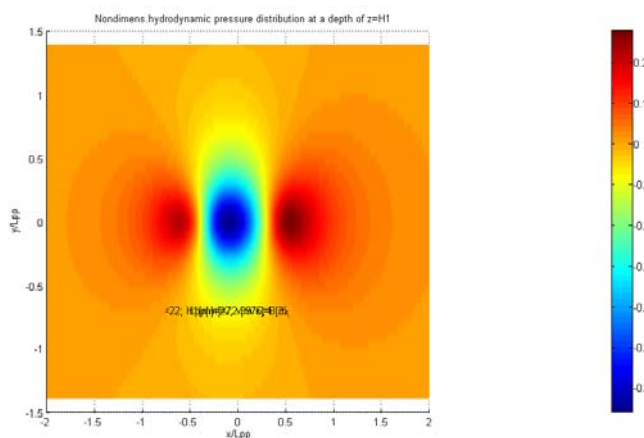


Fig. 14 The hydrodynamic pressure field of *Quest* on a plane Oxy parallel to the bottom of the sea. Ship speed $V_x=6.322\text{m/s}$, with a drifting speed of $V_y=0.1\text{m/s}$.

For the movement of the ship at a drift speed, the low pressure peak grows and differentiates, the level of high pressure increases, and the pressure on the bow and the stern decrease.

5. NONDIMENSIONAL CHARACTERISTICS OF THE SHIP'S HYDRODYNAMIC PRESSURE FIELD

Using the results of measurements and HPF calculations for the three ships, *Zodiak*, *Kapitan Poinc* and *Quest*, the length dependence of low pressure peak depending on the transverse distance from the PS was specified, and from the depths of the sea, H . In dimensionless forms these relationships for the three ships are shown as a function of the dimensionless distance y_{nd} of the PS, as seen in the figure below.

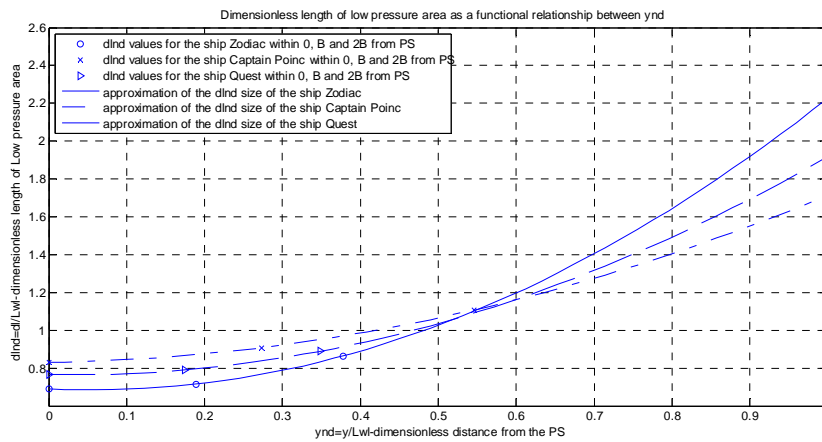


Fig. 15. Dimensionless distance of the low pressure peak as a function of the dimensionless distance y_{nd} of the PS.

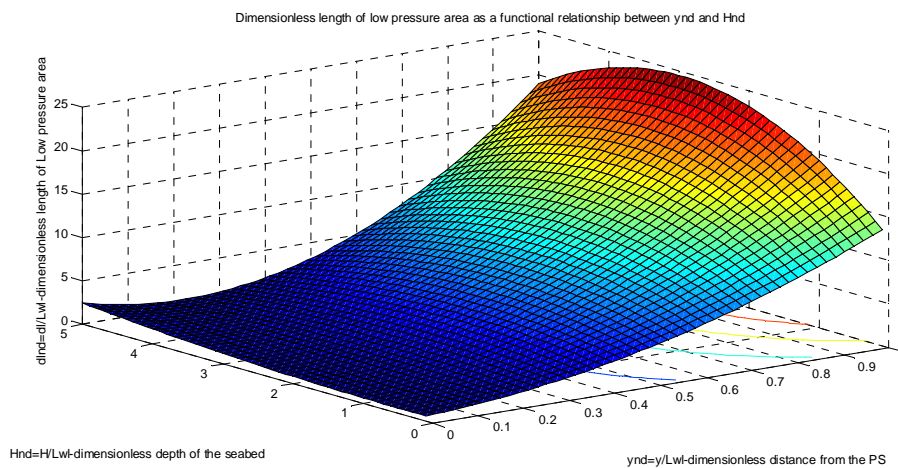


Fig. 16. The surface of the low pressure area length in the dimensionless form in space of $y_{nd} = y/L_{wl}$, and $H_{nd} = H/L_{wl}$.

6. CONCLUSIONS

1. Measurements and HPF calculations for medium vessels with a length of 100m showed very good agreement with the value of the low pressure peak, a slightly smaller length of a low pressure peak, and the largest differences are observed for values of high pressures at the bow and the stern. This confirms this conclusion drawings 6-8 and 10.
2. These differences between the measurements and calculations may explain the much steeper HPF wall surfaces near to the highs, rather than the lows; because during the measurement, the vessel almost never directly passes over the measurement probe, or rather its plane of symmetry is located between the probes. The surfaces with a close approximation of the radius of curvature near the minimum and maximum HPF might lead to the observed differences between measurements and calculations. In other words, the maxima of the measurements could be underestimated.
3. As shown by Figures 11 and 13, the drift speed of the vessel has a significant impact on the value of the low pressure peak and even more on the value of the high pressure at the bow and the stern. Drift speed has virtually no significance concerning the length of the low pressure.
4. Above point (3) may further explain the differences in the measurements and calculations by the presence of even a small drifting speed of the ship.
5. Dividing the hydrodynamic pressure by dynamic pressure and rendering the same into a dimensionless form equal to pressure coefficient C_p , the coefficient C_p is independent of the ship's speed.
6. Using the results of measurements and HPF calculations for these three vessels were defined dimensionlessly according to the length of the low pressure area dl_{nd} in relation to the ship's speed v (Figure 10), and the dimensionless distance from PS y_{nd} , as well as the dimensionless depth H_{nd} (Figure 16). These relationships describe the function of ship-size similar to that of the *Zodiak*, *Quest* and *Kapitan Poinc* :

$$dl_{nd}=f(v,y_{nd},H_{nd}).$$

7. The surface of the low pressure area length in a dimensionless form (fig.16) describes a polynomial function in the form of (1)

$$f(x,y) = p00 + p10*x + p01*y + p20*x^2 + p11*x*y + p02*y^2 + p30*x^3 + p21*x^2*y + p12*x*y^2 + p40*x^4 + p31*x^3*y + p22*x^2*y^2 \quad (1)$$

where $f(x,y)$ [-] and $x= y_{nd}, y = H_{nd}$ and coefficients:

$$p00 = 0.6615, p10 = 2.14, p01 = -0.06718, p20 = 9.733, p11 = 0.7124, p02 = 0.08404, \\ p30 = -2.915e-013, p21 = 7.39, p12 = -0.7658, p40 = -2.071e-014, p31 = 5.715e-014, \\ p22 = -0.668;$$

REFERENCES

- [1] K.J. Bai, R.W. Yeng, Numerical Solution to Free-Surface Flow Problems. 10 th Symposium on Naval Hydrodynamics.
- [2] J. Bielański, Analysis of the hydrodynamic pressure and velocity field flowing around the ship, Scientific and Research Work W.O.i O. PG No. 47/11/PB, Gdańsk 2011, (in Polish).
- [3] R. Canale, S. Chapra, Numerical Methods for Engineers: with Software and Programming Applications, McGraw-Hill, New York, 2002.
- [4] G. Forsythe, M. Malcolm, C. Moler, Computer Methods for Mathematical Computations, Prentice Hall, Englewood Cli@s, 1977.
- [5] T. Inui, Introductory Remarks. International Seminar on Wave Resistance. The Society Of Naval Architects of Japan, 1976.
- [6] M.J. Journée, W.W. Massie, OFFSHORE HYDROMECHANICS. Delft University of Technology, January 2001.
- [7] D. Kahaner, C. Moler, S. Nash, Numerical Methods and Software, Prentice Hall, EnglewoodCli@s, 1989.
- [8] Kozaczka E., Milanowski L.: Badania doświadczalne ciśnienia hydrodynamicznego wytwarzanego przez płynący statek. Prace XII Sympozjum z Hydroakustyki, 179-186, Jurata, AMW, 1995.
- [9] Kozaczka E., Milanowski L., Komorowski A., Czarnecki S.: The application of ship hydrodynamics field distribution for its localisation. Proceedings of the Conference Undersea defence Technology, 397-397, Londyn 1996.
- [10] Kozaczka E., Milanowski L.: Hydrodynamic pressure of a ship. Proceedings of the International Symposium on Hydroacoustics and Ultrasonics, 173-178, Jurata, 1997.
- [11] J.H. Mathews, K.D. Fink, Numerical Methods Using MATLAB, Prentice Hall, Upper Saddle River, NJ, 1999.
- [12] S.S. Rao, The Finite Element Method in Engineering, 3rd ed., Butterworth Heinemann, Boston, 1999.
- [13] B. Średniawa, Hydrodynamics and the theory of elasticity. PWN, W-wa, 1977, (in Polish).
- [14] O.C. Zienkiewicz, R.L. Taylor, The Finite Element Method, 4th ed., Vol. 1, McGraw-Hill, London, 1989.
- [15] Yang, Cao, Chung, Morris, Applied Numerical Methods Using MATLAB, Copyright 2005 John Wiley & Sons, Inc.